Powder Technology 399 (2022) 117207

Contents lists available at ScienceDirect

Powder Technology

journal homepage: www.elsevier.com/locate/powtec

Effect of excipient properties and blend ratio on the compression properties of dry granulated particles prepared from microcrystalline cellulose and lactose

Maryam Tofiq *, Josefina Nordström, Ann-Sofie Persson, Göran Alderborn

Department of Pharmaceutical Biosciences and the Swedish Drug Delivery Forum, Uppsala University, Box 591, SE-751 24 Uppsala, Sweden

ARTICLE INFO

Article history:
Received 19 November 2021
Received in revised form 4 February 2022
Accepted 14 February 2022
Available online 19 February 2022

Keywords:
Dry granulation
Granule composition
Granule strength
Powder compression
Compression parameters
Granule deformation

ABSTRACT

In this study, the effect of a systematically varied excipient ratio of a plastic and a brittle material, i.e., microcrystalline cellulose (MCC) and crystalline α-lactose monohydrate (LAC), on the compression properties of dry granulated particles was investigated. Five powders with different MCC:LAC ratios were prepared by dry mixing; subsequently, they were formed into slugs that were milled and sieved, giving granules of two size fractions. Two slugging pressures were used, giving granules of different porosity for each powder. Original powders and granules were compressed, and strain-pressure profiles determined. From these profiles, a series of compression parameters were derived using the Heckel, Kawakita, and Adams compression equations.

The initial part of the compression profiles of all granulated powders were similar up to a jamming point, after which the compression profiles diverged depending on the granule composition and the slugging pressure. Parameters derived from the Adams and Kawakita equations reflected the differences in compression behavior, while the Heckel parameter did not. The macroscopic compression stiffening was assessed by the Adams friction parameter which seemed to be controlled by the inner friction of the granules, i.e., their plastic deformation due to inter-particulate flow. The total compressibility, assessed by the Kawakita parameter, was dependent on the initial bulk porosity of the granulations.

It is concluded that the composition, microstructure, and packing density of the granules dictated their compression properties, while the granule size and work hardening of primary particles were insignificant.

List of symbols

Symbol	Meaning	Unit
A	Heckel intercept	–
a	Kawakita compression parameter	–
b^{-1}	Kawakita compression parameter	MPa
C	Engineering strain	–
D_s	Slug diameter	cm
E_{bulk}	Total bulk porosity of the granule bed	%
E_H	In die porosity of tablets, Heckel equation	%
E_{extra}	Extra-granular bulk porosity of the granule bed	%
E_s	Geometrical slug porosity	%
F_s	Fracture force of slugs	N
f_{MCC}	Weight fraction of MCC in the powder blend	%
h_0	Initial powder bed, Adams equation	cm
h	Current powder bed, Adams equation	cm
h_s	Slug height	cm
k	Heckel slope	MPa^{-1}
P	Applied pressure	MPa
P_s	Slug pressure	MPa
P_c	Compression pressure	MPa
P_y	Heckel compression parameter: Yield pressure	MPa
S_0	Primary particle specific surface area	cm^{-1}
S_1	Granule specific surface area	cm^{-1}
V_s	Geometrical slug volume	cm^3
α	Adams compression parameter: Pressure coefficient	–
ε_n	Natural strain, Adams equation	–
ρ_{AZ}	Powder bulk density in steel cylinder	g/cm^3
ρ_{app}	Apparent particle density	g/cm^3
$\rho_{g\ bulk}$	Granule bed bulk density	g/cm^3
$\rho_{p\ bulk}$	Powder bed bulk density	g/cm^3
ρ_{eff}	Geometrical slug density	g/cm^3
$\rho_{rel\ g}$	Relative granule density	–
$\rho_{rel\ t}$	Relative tablet density	–
ρ_t	Geometrical tablet density	g/cm^3
σ_s	Tensile strength of slugs	MPa
τ_0	Adams compression parameter: Single granule strength	MPa

1. Introduction

Tablets are the most popular oral solid dosage form, and the final preparation is typically formed by confined powder compression. In

* Corresponding author.
E-mail address: maryam.tofiq@farmbio.uu.se (M. Tofiq).

https://doi.org/10.1016/j.powtec.2022.117207

the manufacturing of tablets, a number of technical demands are placed on a powder that should be compressed into tablets to ensure good manufacturability. Granulation, i.e., the formation of larger particles from finer particles, is frequently used to improve critical technical powder properties, such as flowability and packing density, while the size of the original particles are approximately preserved.

According to the manufacturing classification system [1], two of the major manufacturing routes in current use are based on wet and dry granulation technologies. The use of dry granulation technologies has increased due to its application in continuous manufacturing [2]. During dry granulation, a blend of fine powders is compressed into compacts, which can be of two forms: slugs (large tablets) formed by uniaxial compaction, or sheets or ribbons formed by roller compaction. The compacts thus prepared are subsequently milled into granules which thereafter are mixed with additional excipients and (re)compressed to obtain the final tablets. Hence, tablet making using a dry granulation technology is essentially a double-compression process.

Dry granulation will enhance the flowability and bulk density of the powder, while the ability to be compacted into a tablet may be reduced [3]. Several explanations are proposed in the literature to explain this reduction or loss of tabletability (or reworkability) [4] among which the dominating are work hardening and granule size enlargement. The term work hardening typically refers to an increase in the plastic stiffness of particles caused by plastic deformation; thus, it will be more difficult to plastically deform the primary particles during the second compression process. A concept addressing the importance of primary particle deformation for the tabletability of dry granulated powders [5] is the unified compaction concept, proposing that the final tablet strength depends on the sum of primary particle deformation occurring during the two compaction steps. Thus, if the tablet forming ability of dry granulated powders is dictated by the total primary particle plastic deformation and significant work hardening occurs during granulation, the tabletability of granulated powder will be lower than the original powder. Patel and co-workers [6] reported that the slugging pressure affected both the fracture strength and the tabletability of the granules and concluded that this effect was caused by differences in granule properties rather than by work-hardening of the primary particles and introduced the term granule hardening. It was proposed that different degree of granule hardening during dry granulation gave different porosity and yield strength of the granules which subsequently affected their tabletability, mediated by different tendency to granule fragmentation. Thus, the impact of granule hardening was explained predominantly by a change in granule fragmentation. However, Sun and Kleinebudde [4] later discussed granule hardening also in relationship to granule deformation. It is therefore of interest to further investigate the impact of the formation pressure of ribbons or slugs on the compression properties of the derived granules.

Granules are secondary particles formed from smaller primary particles; hence, granules are porous. Since the primary particles are typically solid, the properties of the granules differ from the original particles not only in dimensions but also in microstructure. Consequently, a granule is, conceptually, a different type of particle compared to a solid particle. Moreover, the microstructure and strength of granules may be critical properties for their compression and compaction properties and thus need to be considered in understanding the loss of tabletability.

By wet granulation technologies, primary particles are bonded together into granules by a liquid, and the force applied to the primary particles is probably considerably lower than during dry granulation. Thus, it is anticipated that the primary particles will typically not deform or fracture during the wet granulation step. Nevertheless, depending on the preparation condition, wet granulated particles can show considerable differences in tablet forming ability; accordingly, primary particle work hardening can hence not explain such differences.

It has been shown [7] that tablets formed of dry granulated particles can show a dualistic pore structure, and it has also been reported that tablets formed from dry granulated microcrystalline cellulose particles [8] had a structure with identifiable granules cohered into a tablet, i.e., the granules tended to remain as secondary particles also after compression. Moreover, it has recently been shown [9] that dry granulated particles may fragment during compression, but these granule fragments were typically larger than the size of the ungranulated particles. The authors also reported that the granule fragmentation occurred predominantly at low compression pressures and that the granule fragments remained intact over the main pressure range. The literature thus provides evidence that a relevant physical model of a tablet formed from dry granulated powders is an aggregate of granules that has undergone fragmentation and deformation during compression. Moreover, the pore structure of such a tablet is principally dualistic with intra- and inter-granular pores (the latter pores also referred to as voids). In comparison, tablets formed of wet granulated particles can also, in many cases, be described as large aggregates of smaller granules [10]. Accordingly, bimodal pore size distributions of tablets formed of wet granulated particles are reported [11] in the literature. It has also been reported that a series of granule properties will be of importance for the compression properties of wet granulated particles, including their porosity [10], strength and plastic stiffness [12], and geometrical shape [13].

Since granules typically consist of a blend of fine powders, it is important to understand how variations in powder composition affect the granule properties, such as their compression properties. The importance of the excipient combination on the compression properties of granules, however, may be complex. Differences in mechanical and intrinsic bonding properties of excipients may affect the granule porosity and strength and possibly also their shape and surface rugosity. Moreover, as pointed out earlier [14], the physical and mechanical properties of the granule forming particles may change due to fragmentation and deformation during the granulation step. Thus, the effect of composition on the compression and compaction properties of dry granules is a complex issue that deserves to be further explored. The objective of this study is to investigate the effects of a systematically varied excipient ratio of a plastic and a brittle material with known different tabletability, i.e., microcrystalline cellulose and crystalline α-lactose monohydrate, on the compression properties of the granules. As descriptors of the compression properties of the granules, some compression parameters were derived by analytical powder compression, and the physical significance of the compression parameters is also discussed. To enable a comparison independent of granule size and size distribution, two narrow sieve cuts of each type of granules were used.

2. Materials and methods

2.1. Materials

Microcrystalline cellulose, abbreviated MCC (Avicel PH 101, FMC Biopolymer, U.S.A.), and crystalline α-lactose monohydrate, abbreviated LAC (Pharmatose 200 mesh, DMV, Veghel, The Netherlands), were used as received. Three binary blends of the two fine powders in the proportions 25:75, 50:50, and 75:25 of MCC:LAC, respectively, were prepared by dry mixing for 5 min in a laboratory shear mixer (QMM-II, Donsmark Process Technology, Denmark) at an impeller speed of 500 rpm. Thus, the five fine powders obtained (two single powders and three blends) were equilibrated for at least three days at a relative humidity (RH) of 40% in a desiccator containing a saturated solution of sodium iodide, at room temperature before further experiments. Magnesium stearate (abbreviated MgSt, Sigma-Aldrich, Sweden) was used as a lubricant.

2.2. Characterization of ungranulated fine powders

The apparent particle density (ρ_{app}) of the ungranulated fine powders was determined by helium pycnometry (AccuPyc II 1340, Micromeritics, U.S.A.). A sample holder of a volume of 10 cm^3 was filled with two-thirds of the powder, and the sample volume was determined

as an average of five consecutive measurements. The reported values are the mean of the measurements of three different samples.

The unsettled bulk density ($\rho_{p\ bulk}$) of the powder bed was determined using a glass cylinder of a diameter of 11.42 mm, resembling the diameter of the tableting die. A sample of powder (about 400 mg) was filled manually inside the glass cylinder, and the sample weight and height, using a height gauge (Mitutoyo, Digimatic 192, Japan), were determined. Moreover, the $\rho_{p\ bulk}$ was calculated as the ratio between the powder bed weight and the volume.

The specific surface area (S_0) of the fine powders was determined by air permeametry using a transient Blaine instrument (in-house made). An amount of powder giving a final powder bed porosity of about 50% was filled into the sample holder and compressed by hand. The specific surface area was calculated by the Kozeny-Carman, corrected for slip-flow and using an aspect factor of 5, as described earlier [15].

2.3. Preparation and characterization of slugs

Slugs were prepared of all five fine powders using a single-punch press (Korsch EK0, Germany) equipped with 15 mm flat-faced punches at two slugging forces of 10 and 20 kN, corresponding to compression pressures of 50 MPa and 100 MPa. A predetermined weight of powder, which gave slugs of approximately 5 mm in height, was individually weighed on an analytical balance for each single slug. The powder was then manually filled into the die and compacted at machine speed. The die was lubricated at regular intervals by compressing a magnesium stearate powder.

For each type of slug, 50 individual slugs were randomly selected, and their height (h_s) and diameter (D_s) were determined using a height gauge (Litematic VL-50A, Mitutoyo, Japan). Thereafter, a geometrical slug volume (V_s) was calculated assuming a cylindrical shape of the slugs, that is:

$$V_s = \frac{\left(\pi D_s^2 h_s\right)}{4} \tag{1}$$

Also, the slug weight was determined using an analytical balance, and the geometrical slug density (ρ_{eff}) was calculated by dividing the slug weight with V_s and finally, a geometrical slug porosity (E_s) was calculated as:

$$E_s = 1 - \frac{\rho_{eff}}{\rho_{app}} \tag{2}$$

The slugs were also individually compressed diametrically in a hardness tester machine (PharmaTest PTB 511E, ISO 9001, Hainburg, Germany) at a linear loading rate increment of 20 N/s, and the force needed to fracture each single slug was recorded (F_s). Thereafter, the tensile strength of a slug was calculated as [16]:

$$\sigma_S = \frac{2F_s}{\pi h_s D_s} \tag{3}$$

2.4. Preparation and characterization of granulated powders

The slugs were milled into granules by hand grinding in a mortar. The granulated powders thus obtained were then sieved using a set of three standard sieves with square openings. The sieve sets were hand shaken for approximately one minute, and two sieve fractions were collected, i.e., 250–500 μm and 500–710 μm. Thereafter, all 10 granulated powders prepared were equilibrated for at least three days at a RH of 40% in a desiccator at room temperature before further experiments.

A steady-state air permeameter was used to assess the enveloped specific surface area of the granulated powders (S_1). About 400 mg of granules were manually poured into a glass cylinder (11.42 mm inner diameter), and the height of the granule bed was measured using a height gauge (Mitutoyo, Digimatic 192, Japan). The glass cylinder was then mounted onto a sample holder that was connected to a pump, and air flow was pumped through the granule bed at a series of controlled flow rates (Brook flow meter, Brook instrument B.V., the Netherlands) between 50 and 2500 mL/min. The generated pressure difference over the bed of granules was recorded by a digital differential manometer (P200 S, Digitron Instrumentation Ltd., U.K.). The specific surface area was calculated by the Kozeny–Carman equation using an aspect factor of 6 [17]. Reported values are the mean of the three measurements.

From the weight and dimensions of the bed of granules, the unsettled bulk density ($\rho_{g\ bulk}$) was calculated as the ratio between bed weight and volume. Thereafter, the extra-granular granule bed porosity (E_{extra}) and the total granule bed porosity (E_{bulk}) were calculated using eqs. 4 and 5. It is here assumed that the geometrical slug density (ρ_{eff}) can be used as an indication of the effective granule density.

$$E_{extra} = 1 - \frac{\rho_{g\ bulk}}{\rho_{eff}} \tag{4}$$

$$E_{bulk} = 1 - \frac{\rho_{g\ bulk}}{\rho_{app}} \tag{5}$$

2.5. Compression of ungranulated and granulated powders

All ungranulated and granulated powders were compressed under a confined condition in a material testing instrument (Zwick Z100, Zwick/Roell GmbH & Co, Ulm, Germany) equipped with a stationary lower and a movable upper punch, both flat-faced and circular with a diameter of 11.3 mm. A 100-kN load cell was used to record the applied force during compression. Before each compression, the die and punch surfaces were brushed with 1% *w*/*v* magnesium stearate suspension in ethanol. After evaporation of ethanol, the pre-lubricated die was filled manually with approximately 400 mg of fine or granulated powder, which was compressed up to an applied pressure of 300 MPa at a linear loading rate of 10 mm/min. For each type of material and tablet pressure, five compressions were done; furthermore, for each compression, the applied force and punch displacement were recorded. The elastic deformation of the materials testing instrument during loading was assessed by pressing the punches against each other ($n = 3$) and a system calibration curve thus derived. The final force-displacement curves of the powders were corrected for this system elastic deformation.

2.6. Analytical powder compression

From the force-displacement curves, strain-pressure profiles were derived, which were also plotted according to the Heckel, Kawakita, and Adams compression equations. From these plots, a series of compression parameters were derived, as described below.

2.6.1. Heckel equation

The expression often referred to as the Heckel equation describes the relationship between porosity reduction and the applied pressure as a first-order kinetic process, that is:

$$\ln\left(\frac{1}{E_H}\right) = kP + A \tag{6}$$

where E_H is the in-die porosity, P the applied pressure, k a material-dependent constant known as the Heckel parameter, and A is the intercept of the linear part of the Heckel plot. The reciprocal of k gives the apparent yield pressure (P_y), which is related to the ability of the material to deform plastically under pressure [18]. Heckel profiles were derived for all powders, and P_y was calculated from data in the pressure range 65 to 280 MPa by linear regression ($R^2 > 0.999$).

2.6.2. Kawakita equation

The Kawakita equation describes the relationship between volume reduction, expressed as an engineering strain, and the applied pressure [19]. The linear form of the hyperbolic equation has the following form:

$$\frac{P}{C} = \frac{P}{a} + \frac{1}{ab} \tag{7}$$

where C is the engineering strain, P is the applied pressure, and a and b are the Kawakita compression parameters. C is calculated as the ratio between $(h_0 - h)$ and h_0, where h_0 is the initial height of the powder bed, while h is the powder height after applied pressure. h_0 was determined by using the unsettled bulk density. The parameter a represents the maximal engineering strain of the powder bed at infinite pressure, whereas the parameter b represents the reciprocal of the pressure needed to achieve an engineering strain of $a/2$ (this parameter is hereinafter reported as b^{-1}). Kawakita profiles were derived for all powders, and the pressure range 20 to 250 MPa was used to calculate the Kawakita parameters by linear regression ($R^2 > 0.999$).

2.6.3. Adams equation

The Adams equation describes the relationship between the volume reduction, expressed as a natural strain, and the applied pressure, that is:

$$\ln P = ln\ \frac{\tau_0}{\alpha} + \alpha\varepsilon_n + \ln\left(1 - e^{(-\alpha\varepsilon_n)}\right) \tag{8}$$

where P is the applied pressure, τ_0 is a parameter representing a failure strength of a single granule, α is a constant related to friction, and ε_n is the natural strain given by:

$$\varepsilon_n = \ln\left(\frac{h_0}{h}\right) \tag{9}$$

where h_0 is the initial height of the powder bed in die, and h is the height of the powder bed at pressure P. At high values of ε_n, the last part of Adams' equation becomes negligible, giving a linear function [20]. Adams' profiles were derived for all powders in the pressure range 2 to 295 MPa, and the Adams parameters τ_0 and α were calculated from data in the pressure range of 10–50 MPa by linear regression ($R^2 > 0.999$).

2.7. Lubrication of granulated powder

Granulated powder prepared at a slugging pressure of 100 MPa and of the size fraction 500–710 μm was mixed with magnesium stearate at two concentrations of the lubricant, i.e., 0.5% and 1% *w*/*w*. A Turbula mixer (Willy A. Bachofen AG, Basel, Switzerland) operating at 22 rpm for 5 min was used. Samples of the lubricated granulated powder were compressed in the materials testing instrument (Zwick Z100) as described in Section 2.5, and the Adams compression parameters τ_0 and α were derived, as described in Section 2.6.3.

2.8. Scanning electron microscopy imaging of powders

Scanning electron microscopy (SEM) images of both starting powders (MCC and LAC) and granulated powders were prepared using a SEM microscope (Zeiss LEO 1530, Carl Zeiss, Germany) operating at an accelerating voltage of 2.0 kV. A sample of each material was mounted on a metal stub using double-adhesive carbon tape. The samples were then sputtered (Polaron SC7640, Quorum Technologies Ltd., U.K.) with gold/palladium under argon gas to enhance the resolution. Images were then taken at 300× and 1000× magnification.

2.9. Data analysis

All graphs and statistical calculations were done in GraphPad Prism 8 for Windows (GraphPad Software, San Diego, California, U.S.A.). All data are presented as mean and relative standard deviation in percent (RSD %).

3. Results

3.1. Ungranulated powder characteristics

The original MCC particles (Fig. 1) were elongated, nearly needle-like with a rough surface containing small open pores, while the original LAC particles had a typical tomahawk shape and a slightly rough but dense surface. The LAC powder consisted of dense crystals while the MCC powder [21] consisted of agglomerates of smaller individual particles (Fig. 1). The importance of the structure of the granule forming particles and the subsequent hierarchical level of the granules for their tableting properties is discussed in the literature [22] and the authors concluded that differences in particle structure may affect the tableting properties of dry granulated powders.

The MCC particles had a slightly higher apparent particle density (ρ_{app}) than the LAC particles (1.574 g/cm^3 and 1.545 g/cm^3 respectively), and the three mixtures had apparent particle densities in-between the starting powders which decreased with increased proportion of LAC (Table 1).

The LAC powder had a higher unsettled bulk density ($\rho_{p\ bulk}$) and higher specific surface area (S_0) than the MCC powder (Table 1). Although the LAC particles were smaller than the MCC particles, they packed more densely; in addition, the lower unsettled bulk density for the MCC powder was likely the result of the more irregular particle shape and the rougher surface texture. The bulk density ($\rho_{p\ bulk}$) decreased gradually, almost linearly, with an increased concentration of MCC (f_{MCC}). The S_0 showed a step-wise dependence on the blend concentration with a marked step from 25% to 75% f_{MCC}.

3.2. Slug characteristics

The slug porosity (E_s) and the slug strength (σ_s) were dependent on both the slugging pressure and the powder composition (Fig. 2). An increased concentration of MCC increased the slug porosity by up to a f_{MCC} of 75% and thereafter levelled out. The magnitude of the increase was dependent on the slugging pressure, i.e., for 100 MPa, the range of E_s was about 20%–23%, while for 50 MPa, the range of E_s was about 24%–35%. The slug strength was strongly dependent on the composition of the powders, i.e., σ_s increased non-linearly with f_{MCC} for both slugging pressures. An increase in slugging pressure from 50 MPa to 100 MPa gave approximately a two-fold increase in σ_s. The difference in σ_s between LAC and MCC is consistent with general knowledge of the compact forming ability of these materials.

3.3. Granulated powder characteristics

Fig. 3 presents the images of granules of only MCC and only LAC, prepared from slugs compressed at 50 MPa and 100 MPa. The images do not indicate any clear difference in the granule geometrical shape. All four types of granules can be described as irregular particles. However, the MCC granules were rougher than the LAC granules. For the MCC granules, the original primary particles can be clearly distinguished, especially for the granules prepared at 50 MPa. For the MCC granules prepared at 100 MPa, the primary particles seemed more deformed, and they were packed closer, making the surface less rough. The LAC granules had a somewhat smoother surface texture with a large number of small particles, indicating that the LAC primary particles fragmented to a significant degree during compression. The LAC granules prepared

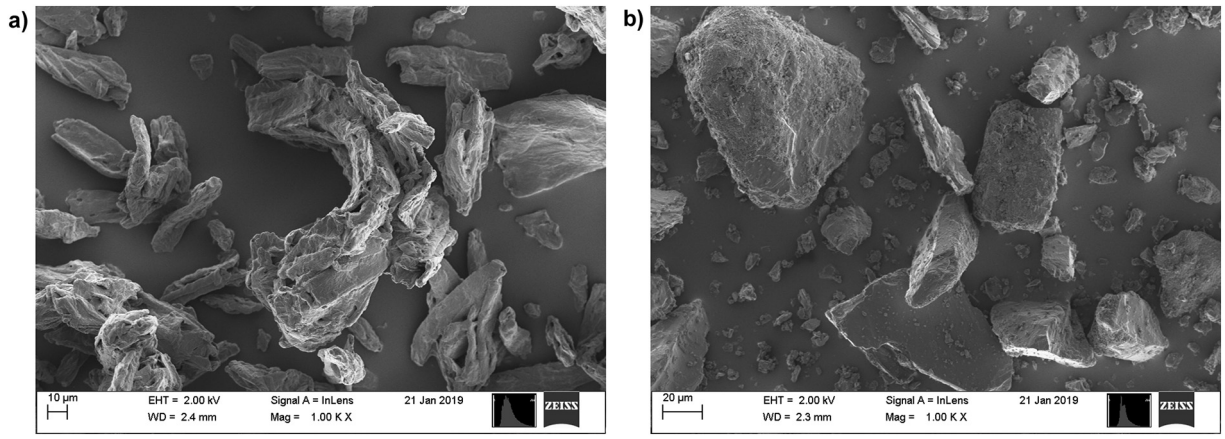

Fig. 1. SEM images of (a) MCC (Avicel PH101) and (b) LAC (Pharmatose 200 mesh) particles.

at 50 MPa seem more porous than the 100 MPa granules, and discrete particles can be distinguished, some of them relatively large.

In Table 2, bulk density ($\rho_{g\ bulk}$), specific surface area (S_1), extra-granular bulk porosity (E_{extra}), and total bulk porosity (E_{bulk}) are reported for all 10 granulated powders. The smaller size fractions had generally, as expected, a higher S_1 than the larger size fraction. However, there was a slugging pressure effect on the surface area, i.e., although consistent sieve cuts were used, granules prepared at the lower slugging pressure had generally a higher S_1 than the granules prepared at the higher slugging pressure.

Granules prepared at the lower slugging pressure (50 MPa) showed generally lower bulk density and higher total bulk porosity than granules prepared at a slugging pressure of 100 MPa. The extra-granular bulk porosity (voidage), however, was independent of the slugging pressure, indicating that the packing density of the granules of the same composition and size fraction was similar. Consequently, the slugging pressure dependent difference in bulk density and total bulk porosity was due to a difference in intra-granular porosity. The larger granules generally had a higher bulk density, a lower bulk porosity, and a lower extra-granular porosity. Thus, the larger granules packed more densely than the smaller granules.

Regarding the composition of the powder, an increased fraction of MCC tended to gradually decrease the bulk density and increase the total bulk porosity. Also, the extra-granular porosity increased slightly with increased f_{MCC}, which can be explained by an increased surface roughness of the granules with increased f_{MCC} (Fig. 3).

3.4. Compression properties of ungranulated and granulated powders

The engineering strain-compression pressure relationships (Fig. 4) initially increased rapidly for both ungranulated and granulated powders and bended thereafter markedly at relatively low compression pressures. Above about 100 MPa, the profiles showed a limited curvature, and they were almost shifted in parallel. For the respective type of powder, the profiles nearly overlapped before the bending but thereafter, the profiles separated and the final degree of compression differed depending on the composition of the powder, i.e., the final degree of compression increased with increased f_{MCC}. The ungranulated powders gave higher final values of engineering strain than the granulated powders, i.e., the compressibility decreased after granulation. For the granulated powders, the compressibility was higher for granules prepared at the lower slugging pressure (the more porous granules), and the smaller granules were more compressible than the larger. The natural strain-compression pressure profiles gave a similar overall pattern as the engineering strain-compression pressure profiles and are not reported here.

For the granulated powders, the pressure-volume relationships were plotted as Kawakita profiles (not shown) and Adams profiles (Fig. 5). The slopes of the linear part of the Kawakita and the Adams profiles differed, depending on the composition of the granules, i.e., an increased f_{MCC} decreased the slope. The Kawakita a parameter, defined as the degree of compression at an infinite pressure, which thus is an indication of the compressibility of the granulated powders, increased with increased $f_{MCC,}$ and the more porous granules had a higher compressibility (Fig. 4 and Table 3). The effect of composition on the b^{-1} parameter was limited, albeit a tendency to an increased value with increased f_{MCC} was obtained.

The Adams τ_0 parameter increased with increased f_{MCC} (Table 3), and the more porous granules gave slightly lower values of τ_0 than the less porous. The larger granules tended to have higher values of τ_0 than the smaller granules, but this was not generally valid. The level of the τ_0 values was generally lower than the slug strengths for a given composition, but the τ_0 showed a similar evolution with f_{MCC} as

Table 1
Particle and powder properties and compression parameters for all ungranulated powders (f_{MCC} denotes the fraction of MCC in the powder). Relative standard deviations in percent (%RSD) within brackets.

Powder	ρ_{app} [a] (g/cm^3)	$\rho_{p\ bulk}$ [b] (g/cm^3)	S_0 [c] (cm^{-1})	P_Y [d] (MPa)	a [e] (−)	b^{-1} [e] (MPa)
0% f_{MCC}	1.545 (0.03)	0.507 (0.15)	8734	170.1 (0.69)	0.659 (0.03)	5.09 (1.36)
25% f_{MCC}	1.562 (0.03)	0.440 (1.73)	8731	145.4 (1.08)	0.713 (0.05)	5.39 (0.61)
50% f_{MCC}	1.565 (0.05)	0.400 (0.39)	6040	120.2 (0.48)	0.747 (0.03)	6.20 (0.90)
75% f_{MCC}	1.569 (0.02)	0.357 (1.51)	5449	98.8 (1.58)	0.784 (0.15)	6.00 (0.65)
100% f_{MCC}	1.574 (0.04)	0.319 (2.16)	5159	83.4 (1.92)	0.810 (0.02)	5.64 (0.64)

[a] Apparent particle density.
[b] Powder bed bulk density.
[c] Primary particle specific surface area.
[d] Heckel compression parameter.
[e] Kawakita compression parameters.

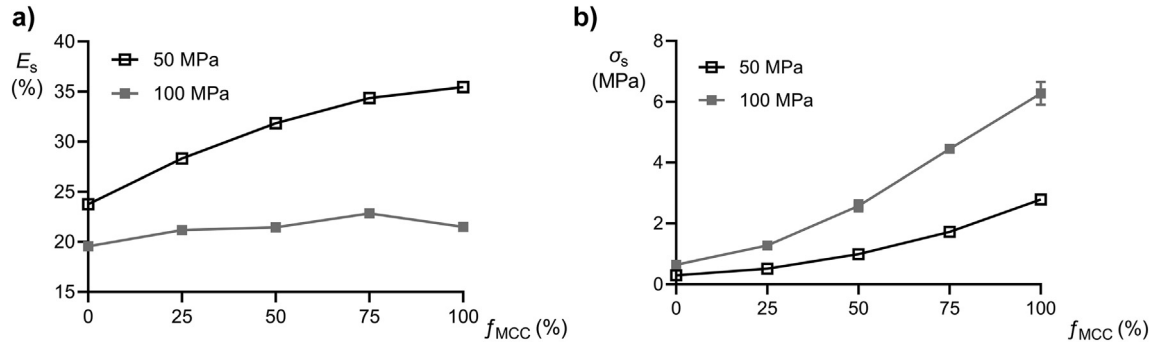

Fig. 2. The effect of powder composition, $\%f_{MCC}$, on (a) porosity, E_s, and (b) tensile strength, σ_s, of slugs prepared at slugging pressures of 50 and 100 MPa.

the slug strength. The Adams α parameter generally decreased with increased f_{MCC} (Table 3), and the more porous granules gave slightly lower values of α than the less porous. Thus, the two Adams parameters related to each other in an inverted way.

The Heckel profiles (Fig. 6) could generally be sub-divided into three regions which is typical for pharmaceutical materials [23], i.e., an initial bended part followed by a nearly linear part that obeys the expression and finally, an up-wards bended part. In all three stages, the composition of the powder affected the relationship. In the first part, the bending of the profile was most marked for the LAC powder; thereafter, the bending gradually became less pronounced with increased concentration of MCC. In the second part, the slope of the plot was lowest for the LAC powder; thereafter, the slope gradually increased with increased concentration of MCC. The difference in the initial bending of the profile between LAC and MCC powder is explained by the higher degree of fragmentation of the LAC, and the difference in slope is explained by a lower plastic stiffness of the MCC powder [24]. The overall shape of the Heckel profiles of the powder mixtures were in-between the profiles of the single powders. For each composition of ungranulated and granulated powders, the Heckel profiles, in contrast to the Kawakita and Adams profiles, gave approximately overlapping relationships over the whole pressure range used.

From the second part of the profiles, the Heckel yield pressure was calculated for all powders and is reported in Tables 1 and 3. The yield pressure decreased almost linearly with increased concentration of MCC for all powders. For each composition, only a limited spread in yield pressures was obtained between the different types of powders, consistent with the similarity in their Heckel profiles. The spread in

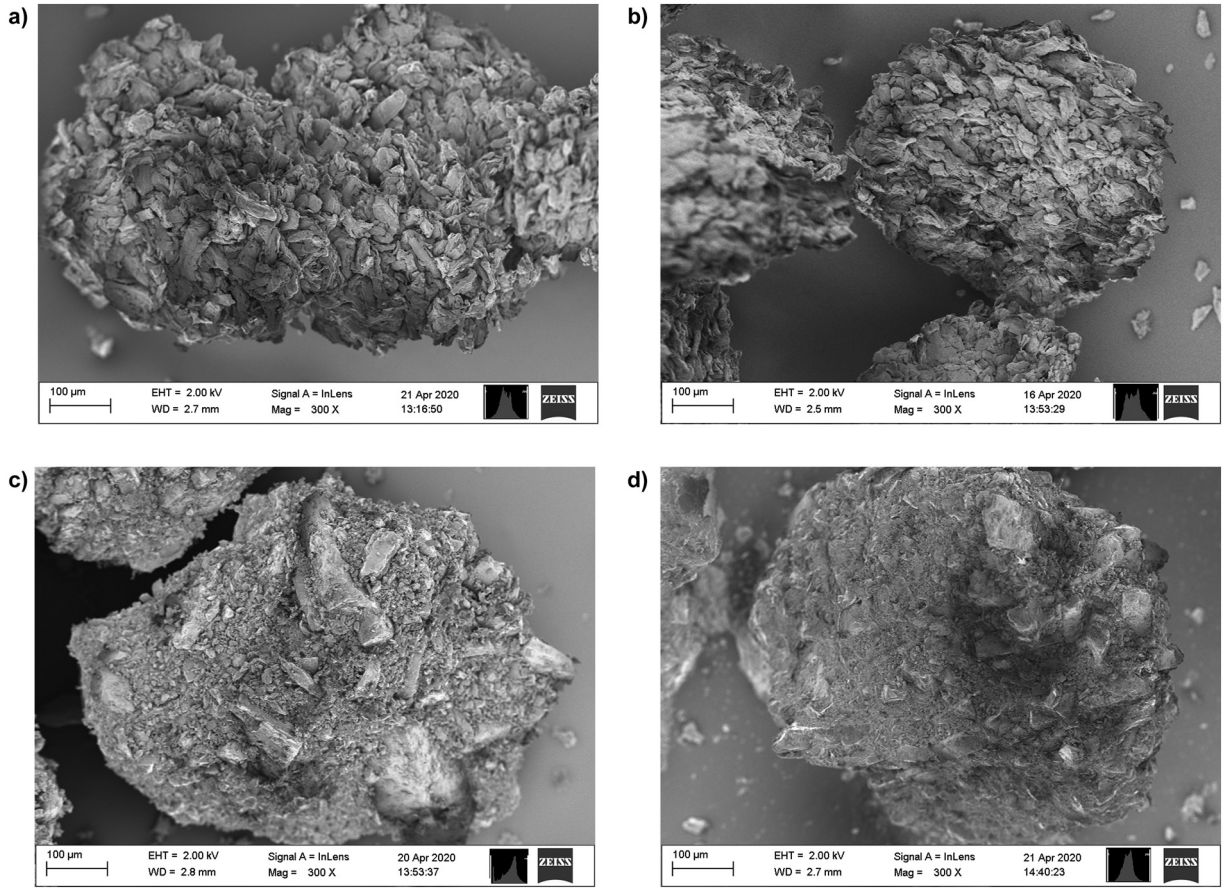

Fig. 3. SEM images of (a) MCC granules prepared at a slugging pressure of 50 MPa, (b) MCC granules prepared at a slugging pressure of 100 MPa, (c) LAC granules prepared at a slugging pressure of 50 MPa, and (d) LAC granules prepared at a slugging pressure of 100 MPa. All granules shown are sampled from the granule size fraction 500–710 µm.

Table 2
Particle and powder properties of the granulated powders (f_{MCC} denotes the fraction of MCC in the powder). The granules were prepared at two slugging pressures (50 and 100 MPa) and with two sieve fractions (250–500 and 500–710 μm). Relative standard deviations in percent (%RSD) within brackets.

Powder	Slugging pressure (MPa)	Granule size fraction 250–500 μm				Granule size fraction 500–710 μm			
		$\rho_{g\ bulk}$[a] (g/cm^3)	S_1[b] (cm^{-1})	E_{extra}[c] (%)	E_{bulk}[d] (%)	$\rho_{g\ bulk}$ (g/cm^3)	S_1 (cm^{-1})	E_{extra} (%)	E_{bulk} (%)
0% f_{MCC}	50	0.59 (2.51)	620 (2.97)	50.0 (2.55)	61.6 (1.57)	0.61 (3.82)	408 (5.19)	48.2 (4.11)	60.5 (2.50)
	100	0.62 (2.76)	539 (6.91)	50.1 (2.74)	59.9 (1.85)	0.65 (2.25)	375 (2.06)	48.0 (2.44)	58.1 (1.62)
25% f_{MCC}	50	0.47 (0.79)	760 (5.13)	57.9 (0.58)	69.8 (0.34)	0.51 (3.44)	481 (5.39)	54.9 (2.83)	67.6 (1.65)
	100	0.53 (2.00)	585 (3.01)	57.0 (1.51)	66.1 (1.03)	0.54 (2.10)	383 (0.02)	56.0 (1.65)	65.3 (1.12)
50% f_{MCC}	50	0.42 (2.80)	801 (6.15)	60.8 (1.81)	73.3 (1.02)	0.43 (0.84)	540 (3.44)	60.0 (0.56)	72.8 (0.31)
	100	0.48 (1.52)	661 (7.64)	61.1 (0.97)	69.4 (0.67)	0.50 (0.61)	457 (2.01)	59.4 (0.42)	68.1 (0.29)
75% f_{MCC}	50	0.38 (1.02)	849 (2.93)	63.2 (0.59)	75.9 (0.32)	0.41 (0.32)	556 (0.43)	60.6 (0.21)	74.2 (0.11)
	100	0.44 (1.10)	703 (3.84)	63.3 (0.64)	71.7 (0.43)	0.46 (0.78)	492 (3.22)	62.0 (0.48)	70.7 (0.32)
100% f_{MCC}	50	0.37 (1.49)	841 (3.84)	63.6 (0.86)	76.5 (0.46)	0.40 (1.21)	558 (1.54)	60.3 (0.80)	74.4 (0.42)
	100	0.44 (2.27)	679 (0.15)	64.7 (1.24)	72.3 (0.87)	0.47 (1.72)	441 (2.93)	62.2 (1.05)	70.3 (0.73)

[a] Granule bed bulk density.
[b] Granule specific surface area.
[c] Extra-granular bulk porosity of granule bed.
[d] Total bulk porosity of granule bed.

yield pressure is not systematic, with one possible exception, which was a higher yield pressure for the LAC granules compared to the ungranulated fine LAC particles.

4. Discussion

4.1. Compression and compaction properties of fine powders

Since granules are small, irregular objects, the mechanical properties of single granules are difficult to reproducibly assess. In this study, the porosity and tensile strength of the cylindrically shaped slugs (briquettes) were used as surrogate measures of the tensile strength and porosity of the granules. The slug porosity ranged from about 20% to about 35% (Fig. 2a), which corresponds favorably with a normal porosity range for ribbons prepared by roller compaction [25]. The relative densities of the slugs were hence considered to be representative of the pharmaceutical ribbons prepared by roller compaction. A positive correlation between ribbon and granule properties has previously been proposed [14]; hence, it is also assumed that the variation in the slug tensile strength corresponds to a similar variation in the tensile strength of the prepared granules.

Both the compression and compaction properties of the starting fine powders (lactose and microcrystalline cellulose) were, as expected, different. MCC had a considerably lower plastic stiffness, as assessed by the Heckel yield pressure, than LAC; moreover, the materials could be described as soft and moderately hard, respectively [26]. The porosity of slugs formed at 50 MPa, however, was higher for MCC than LAC, indicating a much higher elastic recovery of the former during decompression, while for the slugs formed at 100 MPa a similar porosity was obtained (Fig. 2a). For both pressures, MCC gave higher tensile strength, although the slug porosity was higher. Thus, the MCC powder had the ability to form inter-particulate bonds of higher bonding strength than LAC.

A gradual change in powder yield pressure (Table 1), slug tensile strength, and slug porosity was obtained by the variation in the composition of the fine powders. For the 50 MPa series, both tensile strength and porosity varied. However, for the 100 MPa series, the tensile strength varied markedly, but the porosity showed only a small variation (Fig. 2).

4.2. Macroscopic compression behavior of the granules

Several processes [27] are thought to be involved in the compression of granular solids, including events involving the granules and the granule forming particles. It has been proposed that the compression events occurring on the single granule level are sequential [28], i.e., repositioning followed by surface deformation and fragmentation and, finally, geometrical deformation and densification of single granules. This conception was derived from studies on the compression properties of spherical granules formed of a ductile material (microcrystalline cellulose). It was later pointed out that a change in the shape of the granules [13] will increase the fragmentation and attrition of the granules as well as the degree of their deformation. As discussed below, it is proposed that also for the dry granulated particles used in this study, different compression mechanisms dominate or regulate different parts of the compression process.

The strain of a powder bed as a function of compression pressure profile is a basic representation of the macroscopic compression behavior of powders, reflecting the evolution in packing state of the column of granules as a function of applied stress. The strain can be represented in a linear (engineering) form or a natural logarithm form (natural). Here, the linear strain, as a function of the compression pressure, is presented (Fig. 4). The overall character of the corresponding profiles of natural strain as a function of compression pressure (Fig. 5) is similar, and the discussion below is also applicable for these profiles.

The course of the strain-pressure profile was similar, both for the fine powders and for the granulated powders. At low applied pressures, the profiles were characterized by a high and almost constant rate of compression, and all compression profiles more or less coincided irrespective of the composition of the powders. It is reasonable that such a high rate of macroscopic compression is associated with predominantly granule rearrangement in combination with fracturing and attrition and limited local deformation of the granules. These processes dominated the initial compression region and were similar between the different granules. At a certain point, there was a significant macroscopic compression stiffening of the powder bed, causing a marked bending of the strain-pressure plot, i.e., this region was characterized by a gradual and significant decrease in the rate of compression. This macroscopic stiffening was initiated at similar compression pressures (about 2–3 MPa) and at a similar strain (about 0.4) for all the granulated powders and at a somewhat higher strain for the fine powders. The term jammed state is used to describe a state at which particle rearrangement cannot explain further compression of a powder [29]. It is proposed that the macroscopic stiffening began directly after the jamming state was reached, and the compression beyond the jamming point was proceeded predominantly by granule plastic deformation.

For the granulated powders, the jamming point was reached at a similar strain but thereafter, the sharpness of the curvature differed, and the bending occurred at different pressure ranges. The sharpest bending occurred only for the lactose granules, while the most extended bending phase occurred for the MCC granules. Thus, the compression profiles diverged in this phase, and the diversion was clearly dependent on the composition of the granules and the slugging pressure used. With

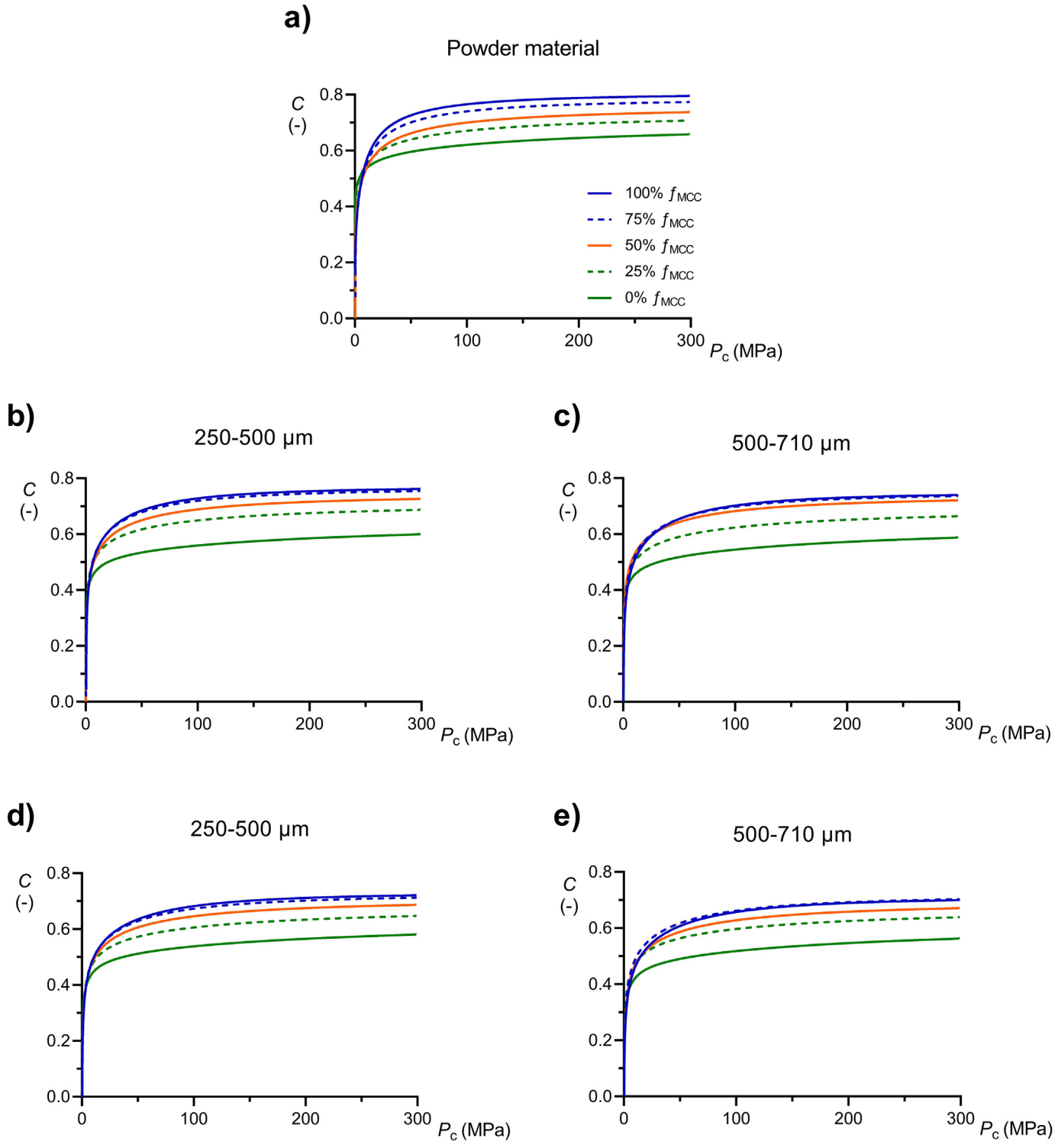

Fig. 4. Engineering strain-compression pressure profiles for (a) ungranulated powders, granulated powders prepared at (b–c) a slugging pressure of 50 MPa, and at (d–e) a slugging pressure of 100 MPa.

further compression beyond pressures of 50–100 MPa, the rate of compression became considerably lower, and the profiles showed only a small curvature which was similar between the powders and independent of their composition. In this upper pressure range, the profiles were shifted in parallel, and the critical part causing the differences in the final degree of compression was the differences in macroscopic stiffening directly beyond the jamming point. In a simplified meaning, the compression profiles could macroscopically be divided into three consecutive phases, and the main differences in compression behavior between the powders were dependent on the evolution of the second phase.

In a recent paper on the fragmentation of lactose and MCC granules prepared by dry granulation [9], it has been reported that granule fragmentation occurred up to a compression pressure up to about 10 MPa and thereafter ceased. The tendency of a single granule to fracture while loaded triaxially [30] has been shown to depend on

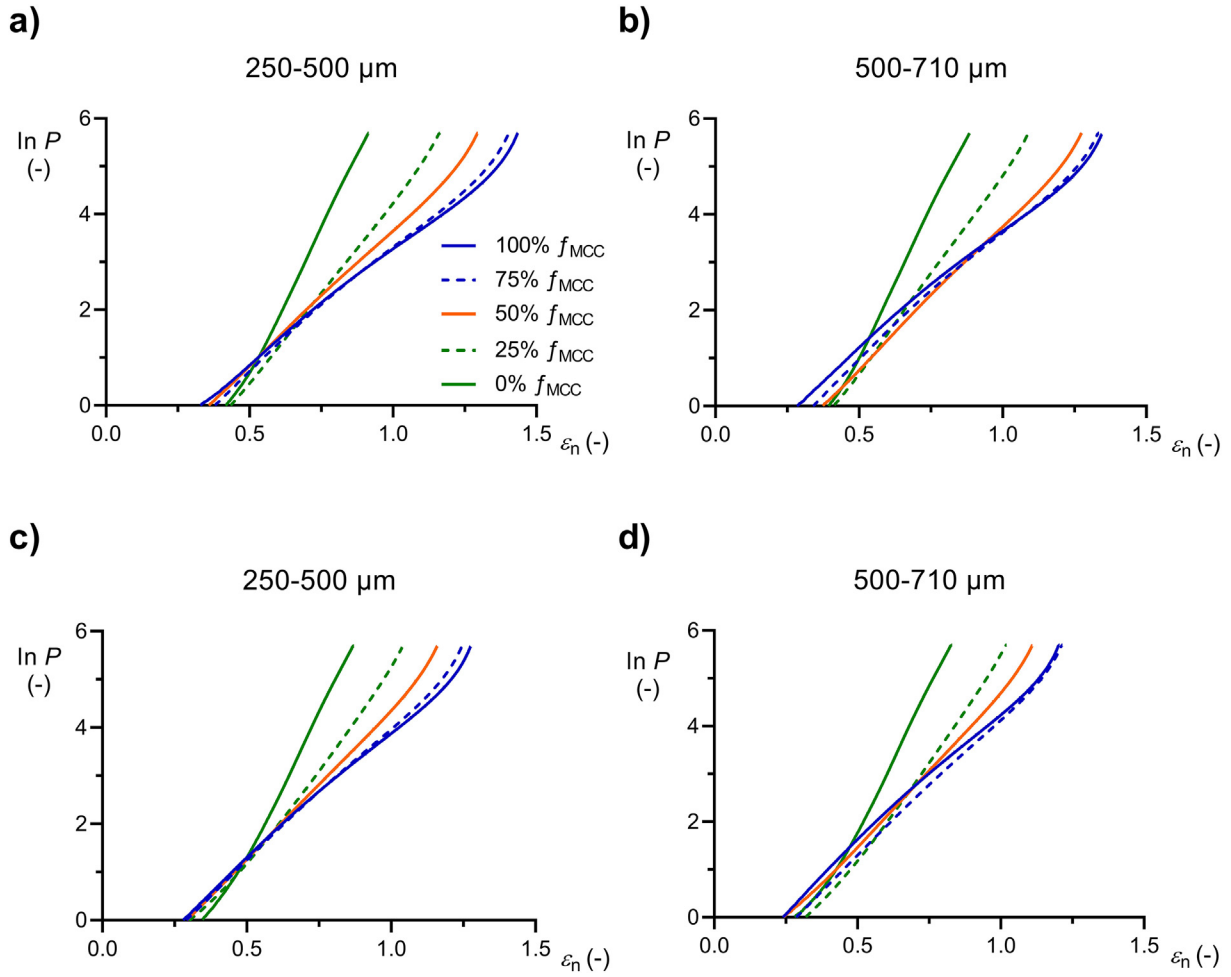

Fig. 5. Compression pressure-natural strain profiles plotted as Adams profiles for granulated powders produced at (a–b) a slugging pressure of 50 MPa and at (c–d) a slugging pressure of 100 MPa.

the triaxiality ratio, i.e., a uniform triaxial loading prevented crack opening and fragmentation of the granules. The reported absence of granule fragmentation at pressures above about 10 MPa may thus be explained by a change in the pressure state of the granules within the die which counteracts and prevents further fragmentation, i.e., a nearly isostatic stress state is quickly reached during compression. In this paper, the first compression phase occurred at a pressure of up to about 2–3 MPa, and the microscopic compression events involved in this phase may hence be predominantly granule rearrangement and some minor degree of fragmentation and local deformation. The continued compression of the powder after the jamming point (phase 2 up to about 50–100 MPa) may initially involve some granule fragmentation but proceeded predominantly by plastic deformation and densification of the granules. Thus, the differences in

Table 3
Compression parameters derived from the Heckel, Kawakita, and Adams equations of the granulated powders (f_{MCC} denotes the fraction of MCC in the powder). The granules were prepared at two slugging pressures (50 and 100 MPa) and with two sieve fractions (250–500 and 500–710 µm). Relative standard deviations in percent (%RSD) within brackets.

Powder	Slugging pressure (MPa)	Granule size fraction 250–500 µm					Granule size fraction 500–710 µm				
		P_Y[a] (MPa)	a[b] (−)	b^{-1} [b] (MPa)	α[c] (−)	τ_0[c] (MPa)	P_Y (MPa)	a (−)	b^{-1} (MPa)	α (−)	τ_0 (MPa)
0% f_{MCC}	50	181.2 (1.36)	0.600 (0.05)	5.96 (1.12)	13.02 (1.09)	0.03 (12.16)	182.5 (0.74)	0.589 (0.06)	6.55 (0.49)	12.93 (0.56)	0.05 (5.23)
	100	185.2 (1.17)	0.582 (0.04)	6.65 (1.08)	12.36 (1.45)	0.09 (11.95)	184.5 (0.73)	0.564 (0.02)	7.32 (0.84)	12.60 (0.78)	0.13 (6.80)
25% f_{MCC}	50	147.1 (0.00)	0.692 (0.02)	5.73 (0.37)	7.44 (0.23)	0.29 (1.42)	149.3 (0.00)	0.669 (0.03)	6.35 (0.66)	7.98 (0.58)	0.33 (4.29)
	100	156.3 (0.00)	0.652 (0.04)	6.61 (0.73)	8.04 (0.52)	0.43 (3.52)	157.2 (0.77)	0.644 (0.04)	6.72 (0.79)	8.54 (0.81)	0.36 (5.99)
50% f_{MCC}	50	111.9 (0.88)	0.737 (0.03)	6.31 (0.97)	5.34 (0.22)	0.98 (1.92)	115.7 (0.57)	0.731 (0.02)	6.34 (0.66)	5.64 (0.19)	0.83 (1.53)
	100	118.8 (0.89)	0.696 (0.05)	7.00 (0.63)	6.05 (0.20)	1.08 (1.46)	125.6 (1.29)	0.681 (0.04)	7.47 (0.42)	6.39 (0.31)	1.11 (2.06)
75% f_{MCC}	50	101.2 (0.76)	0.767 (0.03)	6.30 (0.57)	4.60 (0.21)	1.26 (1.51)	104.8 (1.07)	0.750 (0.01)	7.02 (0.57)	4.79 (0.13)	1.49 (0.83)
	100	99.2 (0.97)	0.726 (0.02)	7.36 (0.35)	5.18 (0.23)	1.58 (3.55)	100.6 (1.21)	0.715 (0.04)	7.59 (0.35)	5.45 (0.19)	1.48 (1.21)
100% f_{MCC}	50	91.1 (0.89)	0.777 (0.03)	6.55 (0.71)	4.29 (0.35)	1.55 (1.80)	90.6 (0.73)	0.757 (0.02)	7.55 (0.56)	4.43 (0.28)	2.03 (1.32)
	100	84.0 (1.19)	0.737 (0.04)	7.70 (0.45)	4.84 (0.29)	1.86 (3.82)	86.4 (0.85)	0.717 (0.03)	8.58 (0.43)	5.02 (0.35)	2.32 (1.49)

[a] Heckel compression parameter.
[b] Kawakita compression parameters.
[c] Adams compression parameters.

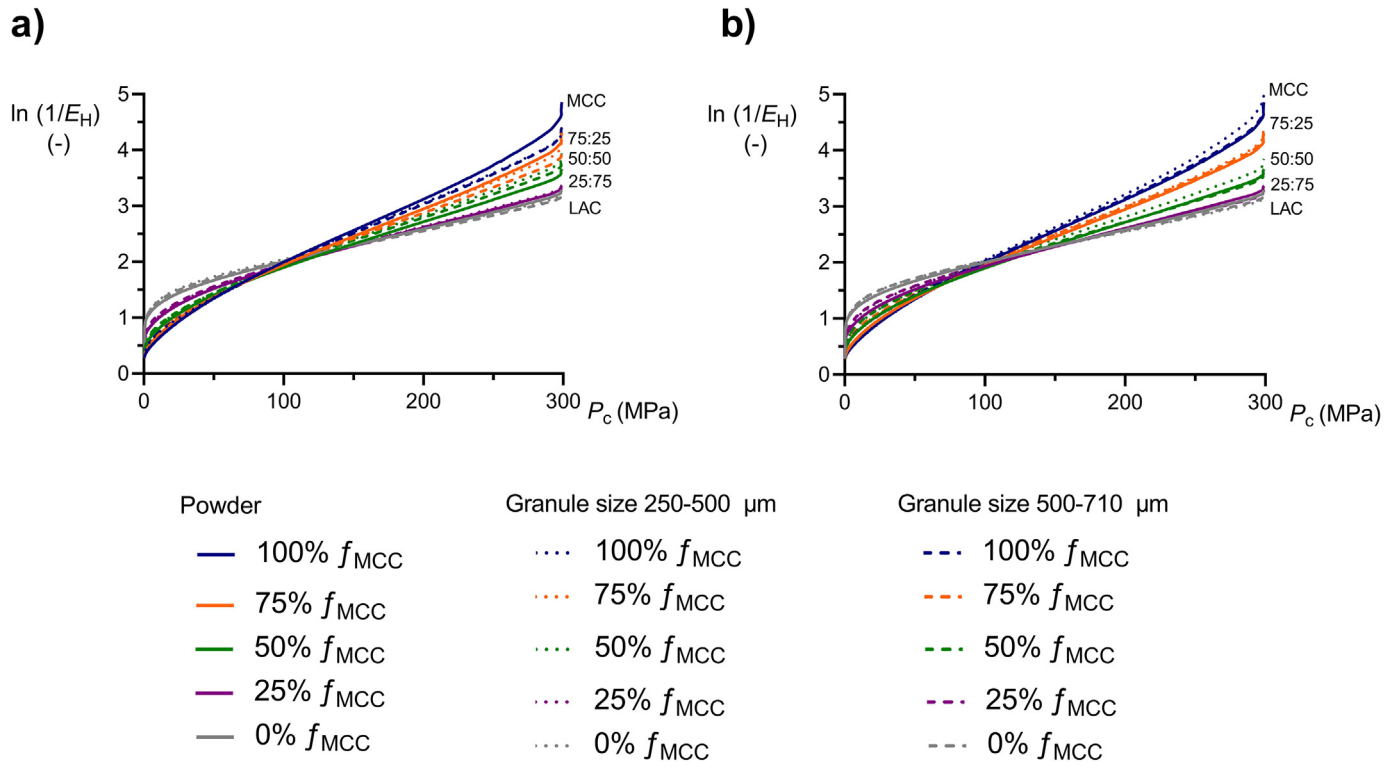

Fig. 6. Heckel profiles of ungranulated and granulated powders prepared at (a) a slugging pressure of 50 MPa and at (b) a slugging pressure of 100 MPa.

macroscopic compression behavior between the granulated powders are dictated by differences in the degree of deformation of the granules.

4.3. Adams parameters

The Adams compression equation [31] is a micro-mechanical compression model with two compression parameters, denoted τ_0 and α. The equation is derived from a column model of powder compression and based on the assumption that the evolution in the number of load-bearing columns with compression pressure is related to the failure of single granules belonging to such columns. This means a failure strength of single granules (τ_0) can be calculated from the slope and the intercept of the linear part of the relationship. This failure strength was originally proposed to be a shear failure, but later [20] alternatively discussed as a tensile failure of the granule. The second parameter (α) is the slope of the linear part of the relationship and was denoted as a pressure coefficient and proposed to be an indication of friction processes occurring during compression, exemplified by the sliding and fracturing of the granules.

The Adams parameters reported in this study were calculated in the compression pressure range of 10–50 MPa. The lower pressure level was chosen to represent a pressure at which granule fragmentation has ceased, in accordance with the findings of Skelbaeck-Pedersen et al. [9]. Above this pressure, it can hence be assumed that further compression of the granule assembly is the result of granule deformation. The upper pressure level was chosen to correspond to the pressure at which the end of the transition phase (phase 2) was approached. The Adams plots (Fig. 5) were almost linear for all granular powders in this pressure range; a range which also covered the main portion of the linear parts of the relationships. Thus, the slope of the Adams plot (the α-parameter) is an indication of the behavior of the granules during the phase of macroscopic compression stiffening beyond the jamming point of all granular powders, i.e., the deformation behavior of the single granules. This parameter was affected by the composition of the granulated powder and the granule strength (Fig. 7).

Since the α-parameter depends on friction processes in the powder, two different friction processes, i.e., friction due to intra-granular flow and friction due to inter-granular sliding, can hypothetically control the course of the macroscopic stiffening. In order to judge the importance of the intra-granular flow and the inter-granular sliding for the α-parameter, Adams parameters were also derived from the compression of a series of pre-lubricated granular powders, i.e., powders anticipated to show lower friction due to inter-granular sliding during compression. The relationships between the pressure coefficient and the composition of the granular powders (Fig. 8a) for the lubricated granular powders and the corresponding unlubricated powders overlapped. It is thus concluded that the intra-granular friction, i.e., the propensity of the granules to deform plastically, is the friction process controlling the macroscopic stiffening of the column of granules.

It has previously been shown [12] that spherical granules composed of a mixture of LAC and MCC had a higher plastic stiffness than granules of only MCC. This is consistent with the finding that the gradient of the linear parts varied depending on the composition of the powders with the highest slope for lactose granules, the lowest for the MCC granules, and the binary mixtures in-between. Moreover, the higher slugging pressure gave granules showing a slightly higher pressure coefficient during compression (Fig. 7a) which also is consistent with the observation [10] that a decrease in granule porosity may decrease the degree of granule plastic deformation expressed during compression. The differences in the sharpness of the bending directly after the jamming point (phase 2) is hence proposed to be related to differences in the plastic stiffness of the granules, dictating the degree of deformation that is expressed during the second phase. In addition, it has also been pointed out [13] that irregular granules are more prone to getting deformed than regular granules and that this may be due to an increased voidage (the inter-granular pore volume) of the bed of granules allowing more deformation. Thus, in addition to granule stiffness, the containment space around the granules in combination with their shape may control the degree to which deformation is expressed.

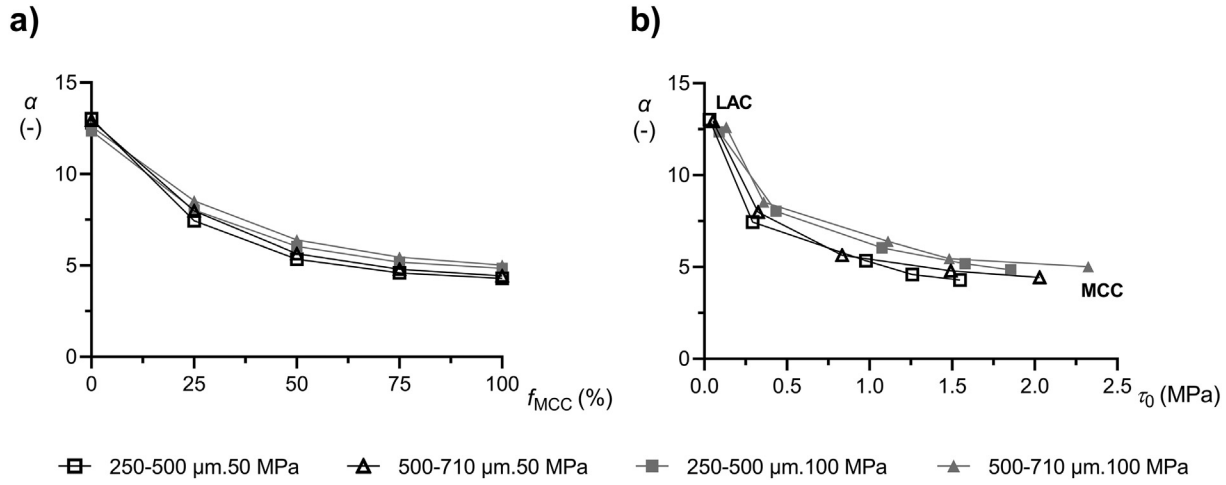

Fig. 7. The effect of granule composition on the Adams parameter α (a) and the relationship between the Adams´ parameters τ_0 and α (b) for all granulated powders.

The Adams τ_0-parameter increased almost linearly with slug strength (Fig. 9), and the relationships originated close to the origin of the axes. The relationship between the τ_0-parameter and the slug strength indicates that this parameter is an indication of the stress needed to fracture individual granules during confined compression [32]. However, the values of τ_0 were considerably lower than the slug strength. The values of the Adams τ_0-parameter reported here for the microcrystalline cellulose granules are also lower than earlier reported for almost spherical pellets of the same material [12,32,33], i.e., about 1 MPa compared to values up to about 35 MPa. Uniyal et al. [34] also reported a value of the Adams parameter of about 1 MPa for dry granulated particles. The difference in failure strength between irregular and spherical granules is explained by their shape difference. In analogy, the strength difference between the granules and the slugs is caused by a shape difference.

An increased τ_0-parameter generally corresponded to a reduced α-parameter (Fig. 7b) in a non-linear way. Also, for the unlubricated and lubricated granules, the relationship between the pressure coefficient and the failure strength (Fig. 8b) overlapped. Thus, for these granular powders, an increased compression failure strength corresponded to an increased plastic stiffness of the granules.

4.4. Kawakita parameters

The Kawakita equation linearized the strain-pressure relationships in an excellent way over a wide range of pressures for both ungranulated and granulated powders. The Kawakita a parameter is the degree of compression of a bed of powder at infinite applied pressure and hence represents an indication of the compressibility of the powder. For the powder used in this study, the granulated powders showed lower compressibility than the ungranulated fine powders. For both ungranulated and granulated powders, a good correlation was obtained between the Kawakita a parameter and the total bulk porosity of the powder before compression (Fig. 10). It is thus concluded that the compressibility was dictated by the relative packing density of the granules in the die before compression and independent of the mechanical properties of the granule forming particles. The macroscopic compressibility of a granular solid is the sum of all compression events occurring at a single granule level, i.e., rearrangement, fragmentation, deformation (plastic and elastic), and densification, which represent the total restructuring of the granule column during compression. It seems that the space allowing for restructuring of the powder during compression is simply the critical property of the granule bed controlling the compressibility. It is also concluded that the morphological nature of the granules is important for the compressibility through an effect on the extra-granular porosity (voidage) of the granule column.

The Kawakita b-parameter is typically presented by its inverted value, i.e., b^{-1}, which is mathematically defined as the pressure needed to achieve a degree of compression of $a/2$. The question of whether this parameter can be interpreted in terms of a physical granule property is discussed in the literature, and it is empirically found that the parameter may correlate with the fracture strength of granules [12,20]. A trend was found that the b^{-1}-parameter increased with slug strength, but the variation in the b^{-1}-parameter was small compared to the variation

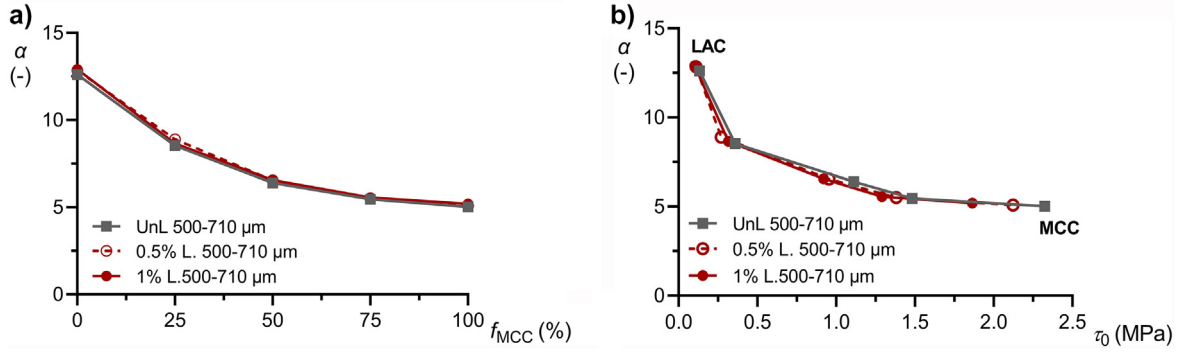

Fig. 8. The effect of granule composition on the Adams parameter α (a) and the relationship between Adams´ parameters τ_0 and α (b) for granulated powders prepared at a slugging pressure of 100 MPa and lubricated externally.

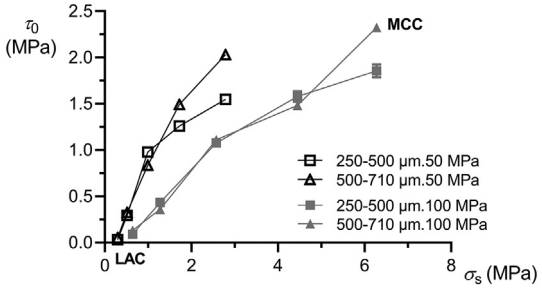

Fig. 9. The effect of tensile strength of slugs (σ_s) on the Adams parameter τ_0 for all granulated powders.

in slug strength. Moreover, there was no correlation between the Adams τ_0-parameter and the b^{-1}-parameter. Thus, for the irregular granules used in this study, the physical significances of the Adams τ_0-parameter and the Kawakita b^{-1}-parameter were different. The Kawakita b^{-1}-parameter probably reflects the rate of compression in the initial compression phase [12] and depends, accordingly, predominantly on two compression mechanisms, i.e., granule rearrangement and fragmentation. The larger granules tended to give somewhat higher values of the b^{-1}-parameter than the smaller granules, which is indicative of the importance of granule rearrangement for the parameter. Thus, the interpretation of the b^{-1}-parameter, in terms of a single granule property, is not meaningful for irregular granules. However, under circumstances where the granule rearrangement is limited and the granule deformation dominates the compression process, it may represent an indication of granule strength or plastic stiffness [12].

4.5. Heckel parameter

Heckel profiles have frequently been used to describe the compression of powders. From such a plot, the Heckel yield pressure is often derived as an indication of the plastic stiffness of the particles. Heckel profiles can be constructed from both the tablet density data after tablet ejection (ex situ data) and from the powder density data under pressure (in situ data). The latter is more commonly used, although it may represent a combined indication of the elastic and plastic stiffness of the particles [35]. Heckel yield pressures have also been derived for dry granulated powders, e.g., Kochhar, Rubinstein and Barnes [36,37]; Hadžović et al. [3]; Šantl et al. [38,39]; Perez-Gandarillas et al. [40]; Freitag and Kleinebudde [41]; and Freitag et al. [14].

The Heckel equation is based on an analogy with a chemical reaction using the concept of reactant pores and change in porosity with pressure increments. As discussed above, a tablet formed of granular solids has a dualistic pore system, comprising pores (within the granules) and voids (between the granules). Johansson and Alderborn [28] showed that different indications of the effective porosity of the powder

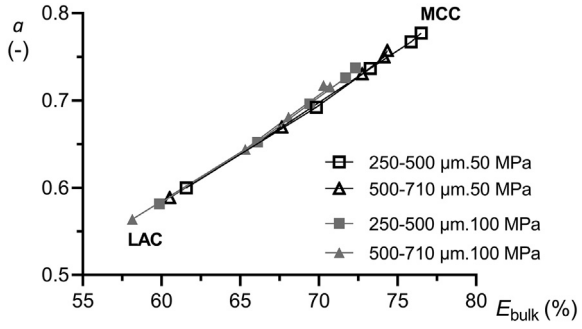

Fig. 10. The effect of the total porosity of the granule bed (E_{bulk}) on the Kawakita a parameter for all granulated powders.

during compression, i.e., the porosity of the voids or the porosity of both pores and voids, will markedly affect the Heckel profiles and hence the derived yield pressures. Later, Persson et al. [33] proposed that the voidage, rather than the global tablet porosity, should be used to approximate the effective porosity of the reactant pores if an estimate of the plastic deformation of the granules is to be determined. Consequently, since Heckel profiles typically, and also in this study, are derived from in situ compression data, estimates of the extra-granular porosity (voidage) cannot be determined. The Heckel profiles cannot be used to assess the plastic stiffness of the granules during compression. The Heckel yield pressure, instead, may represent an indication of the plastic and elastic stiffness of the primary particles forming the granules, rather than the granules. This means that the Heckel approach can potentially be used to probe work hardening of the primary particles during slugging or roller compaction.

For both the fine and granulated powders used in this study, the yield pressure varied systematically with the composition. Similar findings on the effect of composition on the yield pressure have been reported previously during compression of granular solids [36,37,40]. The Heckel profiles for the granulated powders almost superimposed the profiles of the fine powders (Fig. 6). Thus, the yield pressures also derived for the granulated powders were controlled predominantly by the powder composition, i.e., the mechanics of the primary particles. There was a tendency that, for the lactose powders, the slugging caused an increase in yield pressure. It has been shown earlier [42] that a reduction in lactose particle size will increase the yield pressure of the particles. Since the slugging probably fragmented the lactose particles, the increased yield pressure is explained by a reduced lactose particle size.

Perez-Gandarillas et al. [40] reported yield pressures of some powders before and after dry granulation, and only a limited effect of granulation was obtained, which is consistent with the finding reported here. Freitag and Kleinebudde [41] observed a continuous increase in yield pressure with specific roll force during compaction for four magnesium carbonate powders. Magnesium carbonate is a hard material [43], and the increased yield pressure may be due to fragmentation, with a consequent increased yield pressure of the primary particles. Šantl et al. [38] obtained higher yield pressures for dry granulated powders compared to the corresponding direct compression powders for mixtures of lactose and microcrystalline cellulose but without discussing the possible role of particle fragmentation during slugging. Regarding the effect of granule size on the yield pressure, only a limited effect was obtained in this study, which is consistent with earlier reports [38,40]. It is however possible that a critical granule size exists, corresponding to granules of low agglomeration numbers, below which the compression properties of the granules will be significantly different.

The agreement between the yield pressures between fine and granulated powders for the respective composition supports the interpretation that Heckel profiles is controlled predominantly by the mechanical properties of the primary particles and that the derived yield pressure hence represents an indication of the plastic and elastic stiffness of the primary particles rather than the granules. The increase in yield pressure observed for the lactose powders after slugging is proposed to be due to a size reduction of primary particles during the slugging. Consequently, the yield pressures derived in this study indicate that minute work hardening of the primary particles occurred during slugging.

An interesting aspect is that the porosity of the powder columns in-die at the series of compression pressures used are practically the same for the ungranulated and granulated powders of the same composition (Fig. 6) albeit the bulk density - and thus bulk porosity - of the powders were as expected different (Tables 1 and 3). Thus, the initial difference in bulk porosity is eliminated very early in the compression process giving similar porosity-pressure profiles and yield pressures for ungranulated and granulated powders of the same composition. Since the pore structure differs between ungranulated and granulated powders this phenomenon is complex and needs further detailed analysis to be clarified.

5. Conclusions

In this paper, the compression properties of dry granulated particles consisting of a systematically varied excipient ratio of microcrystalline cellulose (MCC) and lactose (LAC) were evaluated using analytical powder compression, i.e., Heckel, Kawakita, and Adams parameters were used. It was found that the compression behavior of the dry granulated particles depended on the composition, the porosity, and the morphology of the granules. The main findings of the study are as follows:

1. Firstly, the compression process involved three phases in sequence, i.e., granule rearrangement and fragmentation until the jamming point was reached followed by a macroscopic stiffening during granule plastic deformation and, finally, ceased bulk compression.
2. Secondly, differences in the stiffening phase were critical for the compression behavior, and the evolution of this phase was markedly affected by the plastic stiffness of the granules. Granule deformation in this critical part of the compression process could be quantified by the Adams α-parameter.
3. Thirdly, the compressibility of the powders, as indicated by the Kawakita a-parameter, was controlled by the original bulk porosity of the granular powder. Thus, all factors affecting the packing of the granules before compression controlled their total compressibility.
4. Fourthly, also for granulated powders, the in situ derived Heckel yield stress parameter indicates the mechanical properties of the solid primary particles rather than the porous granular particles, and the Heckel approach can potentially be used to probe work hardening of the primary particles during slugging or roller compaction.

Declaration of Competing Interest

The authors report no competing interest.

Acknowledgements

This work is part of the science program of Swedish Drug Delivery Forum (SDDF)/Swedish Drug Delivery Center (SweDeliver), and financial support from VINNOVA (Dnr 2017-02690 and Dnr 2019-00048) is gratefully acknowledged. The author would like to thank Irès Van der Zwaan and Sohan Sarangi for assisting in the slugging production. Further thanks to master student Riham El Ammarin for producing the lubrication data, and special thanks to Dr. Lucia Lazorova for taking the SEM images.

References

[1] M. Leane, K. Pitt, G. Reynolds, The manufacturing classification system (MCS) working group, a proposal for a drug product manufacturing classification system (MCS) for oral solid dosage forms, Pharm. Dev. Technol. 7450 (2015) 12–21, https://doi.org/10.3109/10837450.2014.954728.

[2] O. Arndt, P. Kleinebudde, Towards a better understanding of dry binder functionality, Int. J. Pharm. 552 (2018) 258–264, https://doi.org/10.1016/j.ijpharm.2018.10.007.

[3] E. Hadžović, G. Betz, Š. Hadžidedić, S.K. El-Arini, H. Leuenberger, Roller compaction of different pseudopolymorphic forms of theophylline: effect on compressibility and tablet properties, Int. J. Pharm. 396 (2010) 53–62, https://doi.org/10.1016/j.ijpharm.2010.06.009.

[4] C.C. Sun, P. Kleinebudde, Mini review: mechanisms to the loss of tabletability by dry granulation, Eur. J. Pharm. Biopharm. 106 (2016) 9–14, https://doi.org/10.1016/j.ejpb.2016.04.003.

[5] L. Farber, K.P. Hapgood, J.N. Michaels, X. Fu, R. Meyer, M. Johnson, F. Li, Unified compaction curve model for tensile strength of tablets made by roller compaction and direct compression, Int. J. Pharm. 346 (2008) 17–24, https://doi.org/10.1016/j.ijpharm.2007.06.022.

[6] S. Patel, S. Dahiya, C.C. Sun, A.K. Bansal, Understanding size enlargement and hardening of granules on tabletability of unlubricated granules prepared by dry granulation 100 (2011) 758–766, https://doi.org/10.1002/jps.

[7] A.B. Selkirk, D. Ganderton, The influence of wet and dry granulation methods on the pore structure of lactose tablets, J. Pharm. Pharmacol. 22 (1970) 86S–94S, https://doi.org/10.1111/j.2042-7158.1970.tb08585.x.

[8] J. Nordström, G. Alderborn, The granule porosity controls the loss of compactibility for both dry- and wet-processed cellulose granules but at different rate, J. Pharm. Sci. 104 (2015) 2029–2039, https://doi.org/10.1002/jps.24439.

[9] A.L. Skelbæk-pedersen, T.K. Vilhelmsen, J. Rantanen, P. Kleinebudde, The relevance of granule fragmentation on reduced tabletability of granules from ductile or brittle materials produced by roll compaction/dry granulation, Int. J. Pharm. 592 (2020) 120035, https://doi.org/10.1016/j.ijpharm.2020.120035.

[10] B. Johansson, M. Wikberg, R. Ek, G. Alderborn, Compression behaviour and compactability of microcrystalline cellulose pellets in relationship to their pore structure and mechanical properties, Int. J. Pharm. 117 (1995) 57–73, https://doi.org/10.1016/0378-5173(94)00295-G.

[11] J. Nordström, A. Persson, L. Lazorova, G. Frenning, G. Alderborn, The degree of compression of spherical granular solids controls the evolution of microstructure and bond probability during compaction, Int. J. Pharm. 442 (2013) 3–12, https://doi.org/10.1016/j.ijpharm.2012.08.011.

[12] J. Nordström, K. Welch, G. Frenning, G. Alderborn, On the physical interpretation of the Kawakita and Adams parameters derived from confined compression of granular solids, Powder Technol. 182 (2008) 424–435, https://doi.org/10.1016/j.powtec.2007.07.009.

[13] B. Johansson, G. Alderborn, The effect of shape and porosity on the compression behaviour and tablet forming ability of granular materials formed from microcrystalline cellulose, Eur. J. Pharm. Biopharm. 52 (2001) 347–357, https://doi.org/10.1016/S0939-6411(01)00186-2.

[14] F. Freitag, K. Reincke, J. Runge, W. Grellmann, P. Kleinebudde, How do roll compaction/dry granulation affect the tableting behaviour of inorganic materials? Microhardness of ribbons and mercury porosimetry measurements of tablets, Eur. J. Pharm. Sci. 22 (2004) 325–333, https://doi.org/10.1016/j.ejps.2004.04.001.

[15] G. Alderborn, M. Duberg, C. Nyström, Studies on direct compression of tablets X. Measurement of tablet surface area by permeametry, Powder Technol. 41 (1985) 49–56, https://doi.org/10.1016/0032-5910(85)85074-9.

[16] J.T. Fell, J.M. Newton, Determination of tablet strength by the diametral-compression test, J. Pharm. Sci. 59 (1970) 688–691, https://doi.org/10.1002/jps.2600590523.

[17] M. Eriksson, C. Nyström, G. Alderborn, The use of air permeametry for the assessment of external surface area and sphericity of pelletized granules, Int. J. Pharm. 99 (1993) 197–207, https://doi.org/10.1016/0378-5173(93)90362-J.

[18] R.W. Heckel, Density-pressure relationships in powder compaction, Trans. Metall. Soc. AIME 221 (1961) 671–675.

[19] K. Kawakita, K.-H. Lüdde, Some considerations on powder compression equations, Powder Technol. 4 (1971) 61–68.

[20] M.J. Adams, R. McKeown, Micromechanical analyses of the pressure-volume relationships for powders under confined uniaxial compression, Powder Technol. 88 (1996) 155–163, https://doi.org/10.1016/0032-5910(96)03117-8.

[21] R. Ek, G. Alderborn, C. Nyström, Particle analysis of microcrystalline cellulose: differentiation between individual particles and their agglomerates 111 (1994) 43–50, https://doi.org/10.1016/0378-5173(94)90400-6.

[22] S. Grote, P. Kleinebudde, Roll compaction/dry granulation of dibasic calcium phosphate anhydrous-does the morphology of the raw material influence the tabletability of dry granules? J. Pharm. Sci. 107 (2018) 1104–1111, https://doi.org/10.1016/j.xphs.2017.12.003.

[23] C. Sun, D.J.W. Grant, Influence of elastic deformation of particles on Heckel analysis, Pharm. Dev. Technol. 6 (2001) 193–200, https://doi.org/10.1081/PDT-100000738.

[24] I. Klevan, J. Nordström, I. Tho, G. Alderborn, A statistical approach to evaluate the potential use of compression parameters for classification of pharmaceutical powder materials, Eur. J. Pharm. Biopharm. 75 (2010) 425–435, https://doi.org/10.1016/j.ejpb.2010.04.006.

[25] A.V. Zinchuk, M.P. Mullarney, B.C. Hancock, Simulation of roller compaction using a laboratory scale compaction simulator, Int. J. Pharm. 269 (269) (2004) 403–415, https://doi.org/10.1016/j.ijpharm.2003.09.034.

[26] R.J. Roberts, R.C. Rowe, The compaction of pharmaceutical and other model materials - a pragmatic approach, Chem. Eng. Sci. 42 (1987) 903–911, https://doi.org/10.1016/0009-2509(87)80048-9.

[27] J. Van Der Zwan, C.A.M. Siskens, The compaction and mechanical properties of agglomerated materials, Powder Technol. 33 (1982) 43–54, https://doi.org/10.1016/0032-5910(82)85037-7.

[28] B. Johansson, G. Alderborn, Degree of pellet deformation during compaction and its relationship to the tensile strength of tablets formed of microcrystalline cellulose pellets, Int. J. Pharm. 132 (1996) 207–220, https://doi.org/10.1016/0378-5173(95)04373-X.

[29] M. Cárdenas-barrantes, D. Cantor, J. Barés, M. Renouf, E. Azéma, Compaction of mixtures of rigid and highly deformable particles: a micromechanical model, Phys. Rev. E 102 (2020) 1–10, https://doi.org/10.1103/PhysRevE.102.032904.

[30] H. Jonsson, C. Öhman-mägi, G. Alderborn, P. Isaksson, G. Frenning, Crack nucleation and propagation in microcrystalline-cellulose based granules subject to uniaxial and triaxial load, Int. J. Pharm. 559 (2019) 130–137, https://doi.org/10.1016/j.ijpharm.2018.12.064.

[31] M.J. Adams, M.A. Mullier, J.P.K. Seville, Agglomerate compression strength measurement test using a uniaxial confined, Powder Technol. 78 (1994) 5–13, https://doi.org/10.1016/0032-5910(93)02777-8.

[32] F. Nicklasson, G. Alderborn, Analysis of the compression mechanics of pharmaceutical agglomerates of different porosity and composition using the Adams and Kawakita equations, Pharm. Res. 17 (2000) 949–954, https://doi.org/10.1023/A:1007575120817.

[33] A. Persson, J. Nordström, G. Frenning, G. Alderborn, Compression analysis for assessment of pellet plasticity: identification of reactant pores and comparison between Heckel, Kawakita, and Adams equations, Chem. Eng. Res. Des. 110 (2016) 183–191, https://doi.org/10.1016/j.cherd.2016.01.028.

[34] S. Uniyal, L.P. Gandarillas, M. Michrafy, D. Oulahna, A. Michrafy, Analysis of densification mechanisms of dry granulated materials, Adv. Powder Technol. 31 (2020) 351–358, https://doi.org/10.1016/j.apt.2019.10.027.
[35] J.M. Katz, R. Roopwani, I.S. Buckner, A material-sparing method for assessment of powder deformation characteristics using data collected during a single compression–decompression cycle, J. Pharm. Sci. 102 (2013) 3687–3693, https://doi.org/10.1002/jps.23676.
[36] S.K. Kochhar, M.H. Rubinstein, D. Barnes, Slugging and recompression characterisation of some blends of pharmaceutical excipients, Int. J. Pharm. 112 (1994) 225–231.
[37] S.K. Kochhar, M.H. Rubinstein, D. Barnes, The effects of slugging and recompression on pharmaceutical excipients, J. Pharm. 115 (1995) 35–43, https://doi.org/10.1016/0378-5173(94)00250-9.
[38] M. Šantl, I. Ilić, F. Vrečer, S. Baumgartner, A compressibility and compactibility study of real tableting mixtures: the effect of granule particle size, Acta Pharma. 62 (2012) 325–340, https://doi.org/10.2478/v10007-012-0028-8.
[39] M. Šantl, I. Ilić, F. Vrečer, S. Baumgartner, A compressibility and compactibility study of real tableting mixtures: the impact of wet and dry granulation versus a direct tableting mixture, Int. J. Pharm. J. 414 (2011) 131–139, https://doi.org/10.1016/j.ijpharm.2011.05.025.
[40] L. Perez-Gandarillas, A. Mazor, D. Souriou, O. Lecoq, A. Michrafy, Compaction behaviour of dry granulated binary mixtures, Powder Technol. 285 (2015) 62–67, https://doi.org/10.1016/j.powtec.2015.05.003.
[41] F. Freitag, P. Kleinebudde, How do roll compaction/dry granulation affect the tableting behaviour of inorganic materials? Comparison of four magnesium carbonates, Eur. J. Pharm. Sci. 19 (2003) 281–289, https://doi.org/10.1016/S0928-0987(03)00133-7.
[42] S. Pazesh, A. Persson, J. Berggren, G. Alderborn, Effect of milling on the plastic and the elastic stiffnes of lactose particles, Eur. J. Pharm. Sci. 114 (2018) 138–145, https://doi.org/10.1016/j.ejps.2017.12.001.
[43] R.J. Roberts, R. Rowe, The effect of punch velocity on the compaction of a variety of materials, J. Pharm. Pharmacol. 37 (1985) 377–384, https://doi.org/10.1111/j.2042-7158.1985.tb03019.x.

Maryam Tofiq is a PhD student in the Pharmaceutical Technology research group at Uppsala University and in the Swedish Drug Delivery Center (SweDeliver) consortium. She received a M.Sc. degree in Pharmacy from Uppsala University with a degree project in Pharmacokinetics and started doctoral studies at the same university in September 2018. The PhD work focuses on how the microstructure and mechanical properties of agglomerates formed by dry granulation can be controlled by formulation measures.

Josefina Nordström has a PhD in Pharmaceutics from Uppsala University, Sweden, and was appointed associate professor in Pharmaceutics in 2014 at the same university. Her major research interests are within the area of solid oral and inhaled dosage forms, focusing on investigating and understanding the structure-functionality relationships of different particle systems. Such knowledge is fundamental for evaluation of the performance and usability of the particle systems in formulation and manufacture of different types of drug products. Dr. Nordström has published 17 original papers in well recognized journals in the field of pharmaceutics.

Ann-Sofie Persson is a pharmacist and has a PhD in Pharmaceutical sciences from Uppsala University, Sweden. She holds a position as a researcher in Pharmaceutical Technology at the same university. Her main research interests focuses on application of analytical powder compression to be used as a tool in manufacturing of solid drugs. Dr. Persson are in addition co-supervisor for Ph.D. students and regularly supervises undergraduate students.

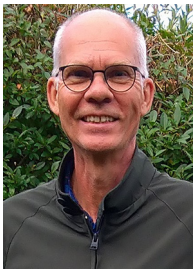

Göran Alderborn has a PhD in Pharmaceutics from Uppsala University, Sweden, and has held the chair in Pharmaceutical Technology at the same university since 1998. His research interest is in the technology and materials science of pharmaceutical powder systems. Current research projects centers on analytical powder compression and on structure - property - performance relationships for granular solids and adhesive mixtures. He has published more than 110 original papers and has contributed to several international text books in the field of pharmaceutics. Prof Alderborn has on numerous occasions acted as reviewer of scientific papers and innovation projects.